CHEMISTRY
A EUROPEAN JOURNAL

DOI: 10.1002/chem.200801263

An Easy Single-Step Synthesis of Platinum Nanoparticles Embedded in Carbon

Sangaraju Shanmugam[a, b] and Ulrich Simon*[a]

Platinum nanoparticles have gained a huge impact towards catalytic processes in science and technology.[1] In conjunction with a solid support they are applicable for technical processes, for example, fuel cell applications. What is most desirable for such applications is the control of the particle size as well as the preferential formation and orientation of certain crystallographic facets, which affect the catalytic performance.[6] While the preparation of catalytically active Pt nanoparticles on solid supports is established utilizing chemical reduction,[2] involving surfactants as protective agents[7] or sol–gel processes,[9] by sonochemical[3]or microwave processes[4] or by chemical deposition techniques,[5] precise control over the particle size, shape and orientation on the support still remains a great challenge.

When prepared through a chemical pathway, supported Pt nanoparticles are typically obtained following a two-step protocol. This involves the deposition of molecular or ionic precursors, such as chloroplatinic acid (H_2PtCl_6), on the desired support from the aqueous or organic liquid phase, followed by the reduction with suitable reducing agents, such as hydrogen, hydrazine or formaldehyde. Limitations of these methods are: i) If H_2 is used, high temperatures (300–500 °C) are usually necessary. Under such harsh reaction conditions the support has to retain its structure and activity. Furthermore, this method can lead to the formation of larger aggregates of the initially well dispersed Pt nanoparticles. ii) Application of formaldehyde or hydrazine as a reducing agent often results in incomplete reduction and is therefore inefficient with respect to the noble-metal load.

[a] Dr. S. Shanmugam, Prof. U. Simon
Institute of Inorganic Chemistry, RWTH Aachen University
Landoltweg 1, 52056 Aachen (Germany)
Fax: (+49) 241-809-9003
E-mail: ulrich.simon@ac.rwth-aachen.de

[b] Dr. S. Shanmugam
School of Advanced Science and Engineering
Waseda University, 3-4-1 Okubo
Shinjuku-ku, Tokyo 169-8555 (Japan)

Supporting information for this article is available on the WWW under http://dx.doi.org/10.1002/chem.200801263.

Thus, the development of synthetic routes allowing catalyst fabrication in direct conjunction with the desired support in one single step is highly desirable. Examples for the preparation of nanoparticles in direct conjunction with a carbon support are given by Zhang et al. and Yu et al.: Zhang et al. reported on the fabrication of platinum nanoparticles embedded in carbon nanofibers by polymerization of acrylnitrile in the presence of platinum acetylacetonate in a porous alumina template.[10] Yu et al. described the facile one-pot synthesis of Se/C composites by taking advantage of microwave heating and hydrothermal effects at a reasonable low temperature. These composites consist of dandelion-like Se nanorod aggregates as the core and amorphous carbon as the encapsulating shell.[11] Such Se/C core–shell nanocomposites have further been employed as a template to fabricate hollow carbon capsules. Recently, Wei et al., developed a facile solution phase hydrothermal route to synthesize Fe-Ni@carbon nanostructures.[12]

In this work we introduce a template-free single-step route for the synthesis of spherical Pt nanoparticles embedded in carbon. This method is facile, solvent-, catalyst-, and template-free and it is easy to handle, and thus might even be scalable. The reaction products were characterized by scanning electron microscopy (SEM), energy dispersive X-ray analysis (EDX), transmission electron microscopy (TEM), X-ray photoelectron spectroscopy (XPS), micro-Raman spectroscopy as well as electrochemically. We will show that the product only consists of carbon and Pt without any other impurities, and that the Pt nanoparticles are chemically accessible in an electrochemical environment.

The Pt–C composite was synthesized using Swagelok stainless steel union parts.[13] For a typical synthesis, 0.5 g of the precursor was introduced into a 5 mL Swagelok reactor cell. The $^3/_4$ inch cell closed from both sides by standard caps. The filled reactor is kept inside the iron pipe, which was placed at the center of the furnace. The temperature of furnace was raised at a heating rate of 25 °C per minute up to the desired reaction temperature, that is, 400 and 500 °C, respectively. The products synthesized at these temperatures are designated as Pt-C-400 and Pt-C-500, respectively. The

XRD patterns of Pt-C-400 and Pt-C-500 are shown in Figure 1. The diffraction peaks can readily be indexed to cubic Pt (JCPDS card 04-0802). For both materials the diffraction peaks were observed at $2\theta = 39.81$, 46.28, 67.63 and 81.37°. These peaks are assigned to the (111), (200), (220), and (311) reflection planes of the face-centered cubic phase of Pt. Applying the Scherrer equation[14] by analyzing the full-width at half maximum diffraction peak of (111) the average particle size of Pt was determined to be 4 nm. The carbon content in Pt-C-400 and Pt-C-500 was 17.5 and 20.1 wt%, respectively, as determined by C, H, and N elemental analysis. The total yield of the Pt-C-400 and Pt-C-500 products was 65 and 58%, respectively (relative to the starting material).

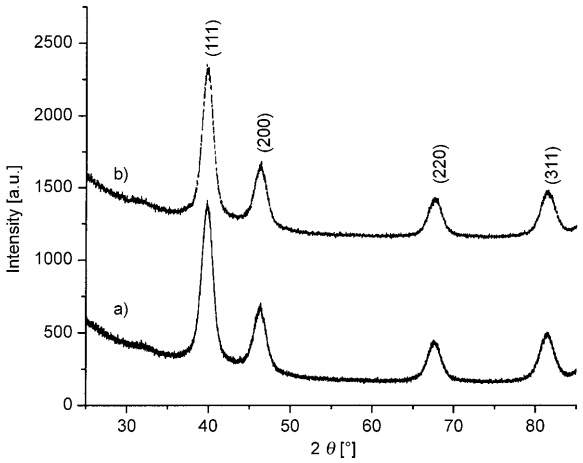

Figure 1. XRD patterns of a) Pt-C-400 and b) Pt-C-500.

The calculated carbon content in the precursor is 30.5%. We assume that the loss of carbon may be due to partial oxidation of carbon to CO and CO_2. Figure 2 shows the SEM image of the two products. The overall morphology mostly exhibits spherically shaped particles with an average diameter of 1.5 μm. In Pt-C-500 the particles are partially sintered, which may be due the higher temperature (Figure 2c).

The EDX spectrum of an individual sphere of Pt-C-400 is given in Figure 2d, which shows Pt and carbon without any other impurities, and proves the purity of the product.

Figure 3 shows the TEM images of Pt-C-400 and PT-C-500. The individual Pt nanoparticles are coated with carbon, which is depicted in Figure 3a by arrows. A histogram of the size distribution of the particles for Pt-C-400 is calculated by counting 200 particles (see Supporting Information). The average particle size is 5.4 ± 1 nm. Thus, the size of Pt particles in both materials ranges between 4 and 6 nm, and they are found to be of crystalline nature, which can be derived from the lattice fringes. The distance measured between the (111) lattice planes is 0.225 nm, which is very close to the distance between the planes reported in the literature (0.228 nm) for the face-centered cubic lattice of the Pt (JCPDS 04-0802). To verify the presence and nature of

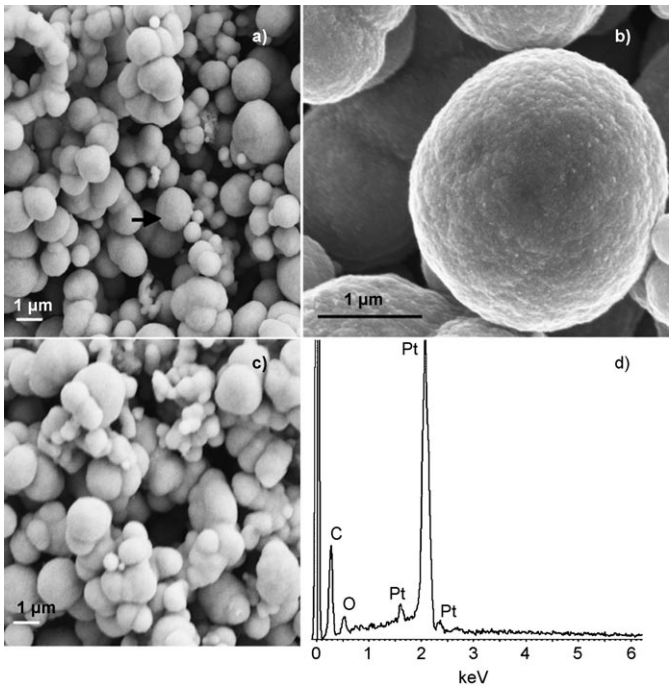

Figure 2. a) SEM image of Pt-C-400, b) SEM image at higher magnification of an individual Pt-C particle marked with an arrow in a), c) SEM image of Pt-C-500 and d) EDAX of Pt-C-400.

carbon in the Pt–C samples we performed Raman spectroscopy. The Raman spectra (see Supporting Information) of Pt-C-400 exhibit two broad peaks at around 1341 (D band) and 1611 cm^{-1} (G band). The G band corresponds to the symmetric E_{2g} vibrational mode in graphite-like structures and is attributed to graphite-like sp^2 microdomains in the products, while the D band corresponds to disordered sp^2 microdomains.[15] Pt-C-500 showed corresponding peaks at around 1343 and 1606 cm^{-1}, respectively, but with higher intensity and lower full-width at half maximum. Hence, the Raman spectra indicate a certain amount of amorphous carbon besides graphitic domains.

This agrees well with the results of the XPS analysis, which was applied to analyze the chemical surface composition with respect to the oxidation states of Pt and the nature of oxygen. The only elements detected on the surface were carbon, platinum and oxygen. The respective concentrations in Pt-C-400 are found to be 75.3 (Pt), 19.5 (C) and 5.2% (O), respectively. The XP spectrum of Pt 4f in Pt-C-400 showed a doublet of Pt $4f_{7/2}$ and $4f_{5/2}$ with the binding energy centered at 71.7 and 75.0 eV, respectively, which suggests that the Pt is in a metallic state.[16]

Figure 4 shows the high resolution XP spectra of Pt-C-400, where the C 1 s spectrum (Figure 3 a) has been deconvoluted into two symmetric peaks (284.8, 285.2 eV) and an asymmetric one (286.2 eV). The main peak (284.8 eV) originates from the C–C and C–H forms of graphitic carbon. The peaks at 285.2 and 286.2 eV can be assigned to sp^3-hybridized carbon atoms bound to one or two oxygen atoms, respectively, whereas the electronegative oxygen atoms

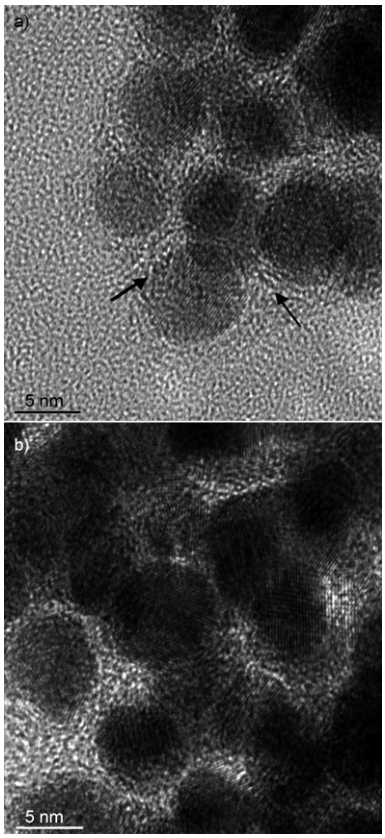

Figure 3. TEM images of a) Pt-C-400, b) Pt-C-500 showing the platinum nanoparticles embedded in carbon.

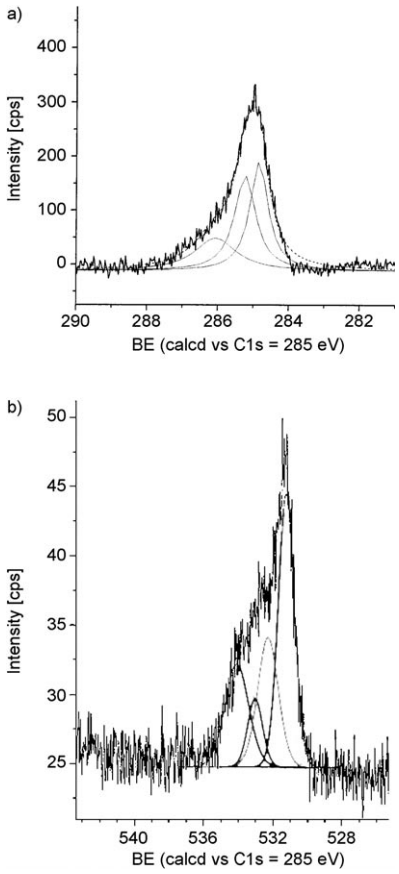

Figure 4. High-resolution XPS spectra of Pt-C-400 a) C 1s and b) O 1s region.

induce a positive charge on the carbon atom. Hence, they can be assigned to alcoholic, ether (C–O) and ketone/aldehyde (C=O) species.[17] The oxygen spectrum in Figure 4b gives four peaks after a similar fitting procedure: One peak at a binding energy of 531.2 eV corresponding to the double bonded oxygen (like C=O group), and peak at 532.3 eV, which is attributed to single bonded oxygen atoms (e.g. C–OH). The two peaks at 534.1 and 533.0 eV could be attributed to the presence of adsorbed moisture and oxygen, respectively.[18]

We can only speculate about the mechanism at this point as to how the carbon embedded Pt nanoparticles are formed. We assume that in a first step upon heating the thermal decomposition of the precursor takes occurs at a temperature above 250 °C, where Pt vapour is formed. The next stage thus seems to be the formation of metallic Pt particles upon vapour nucleation and condensation, followed by the coagulation of particles. At the same time carbon monoxide is released from ligand decomposition, which may undergo catalytic disproportionation to form carbon and CO_2 through the Boudouard reaction.[19] It is observed that the disproportionation reaction of CO takes place around 330 °C on Pt.[20] Then, the mirostructure of final product is determined during the cooling and is related to carbon segregation in the supersaturated particles due to the reduction in solubility as the system's temperature decreases.[21] If the cooling rate would be infinitely slow, the particle structure achieved after carbon segregation would be graphitic carbon around the Pt particles, which is regarded as the equilibrium structure. However, due to competition between the segregation and surface fluxes, two situations can occur in the system upon cooling. It may form a carbon core and Pt shell or a Pt core with carbon shell. It is known that the crystallization of Pt is faster than that of carbon; thus, first Pt crystallizes first giving rise to the carbon coating on the Pt nanoparticles.

In order to analyse the chemical accessibility of the embedded Pt nanoparticles we studied the electrochemical properties of Pt-C composites (see Supporting Information). The cyclic voltammograms were obtained in aqueous 0.5 M H_2SO_4 at a sweep rate of 25 mV s^{-1}. The voltammetric features of Pt-C-500 composites are characteristic of Pt metal, with Pt oxide formation in the + 0.60 to +1.20 V region, the reduction of Pt oxide at about +0.40 V, and the hydrogen adsorption (−0.054 V) and desorption (−0.112, 0.025 V) peaks. In Pt-C-400, the hydrogen adsorption and desorption peaks are observed at −0.064 and +0.021 V, respectively. The Pt oxide formation was observed at higher potential range and the reduction of Pt oxide at +0.388 V. These observations suggest that the nature of carbon affect the elec-

trochemical properties of Pt–C composite electrode, and furthermore that the Pt particles are chemically accessible and in good electronic contact with the carbon surface.

In summary we introduced a simple and easy method for the preparation of carbon supported 4–6 nm Pt nanoparticles by thermal decomposition of $Pt(acac)_2$ at 400 and 500 °C, respectively. The content of amorphous carbon was found to be higher in the materials synthesized at higher temperature, as confirmed by Raman spectroscopy. We demonstrate that these particles are electrochemically active, and hence, chemically accessible for catalytic reactions. The described route is simple and elegant, and we assume that it will be suitable for the preparation of other catalytically active metal/carbon composites.

Experimental Section

Synthesis: Platinum(II) acetylacetonate was purchased from Aldrich with a purity of 99%. Platinum(II) acetylacetonate (0.5 g) was filled into the Swagelok cell at room temperature under atmospheric conditions. The cell was closed tightly and then placed at the center of the furnace. The temperature was raised at a heating rate of 25 °C per minute up to a temperature of 400 °C, where it was held for 3 h. The reaction took place under the autogenic pressure of the precursor. The closed cell heated to 400 °C was gradually cooled to room temperature, opened with the release of a little pressure. The product synthesized at 400 and 500 °C are designated as Pt-C-400 and Pt-C-500, respectively.

Analysis: Scanning electron microscopy (SEM) of the obtained product was carried out on a field emitter SEM LEO Supra 35VP with in lens detector combined with an Oxford Instruments EDX INCA Energy 200 (133 eV, SiLi detector). The particle morphology was studied with transmission electron microscopy on a JEOL-JEM 100 SX microscope, working at a 100 kV accelerating voltage, and a FEI Tecnai F20, with an accelerating voltage of 200 kV. Samples for TEM were prepared by ultrasonically dispersing of the products in absolute ethanol, placing a drop of this suspension onto a copper grid coated with an amorphous carbon film and then drying under air. Powder X-ray diffractograms were recorded in the range $20° < 2\theta < 80°$ on a STOE STADIP diffractometer using $Cu_{K\alpha 1}$ radiation (40 kV, 30 mA) and a germanium monochromator. The elemental analysis of the sample was carried out by an Eager C, H, N, S analyzer. The Perkin–Elmer system 2000 Raman spectrometer was employed, using the 514.5 nm line of an Ar laser as the excitation source to analyze the nature of the carbon present in the products. XPS measurements were performed in ultrahigh vacuum (UHV) with Kratos, axis HS monochromatized $Al_{K\alpha}$ cathode source, at 75–150 watt, using low energy electron plod gun for charge neutralization. Survey and high resolution individual metal emissions were taken at medium resolution, with pass energy of 80 eV, and steps of 50 meV.

A single glass compartment, three-electrode cell was employed for the cyclic voltammetry. Pt wire and saturated calomel electrodes (SCE) were used as counter and reference electrodes, respectively. A 0.076 cm^2 area glass carbon (GC) served as the working electrode. The electrochemical studies were carried out with a CH I 630 Electrochemical analyzer (CHI Instruments Inc. USA). Pt–C (15 mg) was dispersed in water (0.5 mL) for 20 min in an ultrasonicator. The dispersed Pt–C (20 μL) was placed on GC and dried in an oven at 90 °C for 2 min. 5% Nafion (5 μL) was dropped on GC and dried at room temperature. The solvent was evaporated, and the Nafion acted as a binder to hold the sample to the electrode. The electrolyte was degassed with nitrogen before the electrochemical measurements.

Acknowledgements

The authors thank Dr. Michael Noyong for SEM-EDX analysis and Dr. Alla Sologubenko for TEM measurements. We extend our thanks to Dr. W. Tillman for Raman analysis and to Dr. Melanie Homberger for helpful discussions.

Keywords: carbon · electrochemistry · heterogeneous catalysis · nanomaterials · platinum

[1] F. Raimondi, G. G. Scherer, R. Koetz, A. Wokaun, *Angew. Chem.* **2005**, *117*, 2228–2248; *Angew. Chem. Int. Ed.* **2005**, *44*, 2190–2209.
[2] a) Z. Zhou, S. Wang, W. Zhou, G. Wang, L. Jiang, W. Li, S. Song, J. Liu, G. Sun, Q. Xin, *Chem. Commun.* **2003**, 394–395; b) H. Li, G. Sun, Y. Gao, Q. Jiang, Z. Jia, Q. Xin, *J. Phys. Chem. C* **2007**, *111*, 15192–15200.
[3] T. Fujimoto, S. Terauchi, H. Umehara, I. Kojima, W. Henderson, *Chem. Mater.* **2001**, *13*,1057–1060.
[4] Z. Liu, X. Yi, X. Ling, Su, J. Y. Lee, *J. Phys. Chem. B* **2004**, *108*, 8234–8240.
[5] P. Serp, R. Feurer, Y. Kihn, P. Kalck, J. L. Faria, J. L. Figueiredo, *J. Mater. Chem.* **2001**, *11*, 1980–1981.
[6] a) I. Balint, A. Miyazaki, A. Ken-Ichi, *Appl. Catal. B Environ.* **2002**, *37*, 217–219; b) M. J. Hostetler, J. E. Wingate, C.-J. Zhong, J. E. Harris, R. W. Vachet, M. R. Clark, J. D. Londono, S. J. Green, J. J. Stokes, G. D. Wignall, G. L. Glish, M. D. Porter, N. D. Evans, R. W. Murray, *Langmuir* **1998**, *14*,17–30.
[7] G. Viau, R. Brayner, L. Poul, N. Chakroune, E. Lacaze, F. Fiévet-Vincent, F. Fievet, *Chem. Mater.* **2003**, *15*, 486–494.
[8] Y. Zhou, S. H. Yu, Y. W. Cui, X. G. Li, Y. R. Zhu, Z. Y. Chen, *Adv. Mater.* **1999**, *11*, 850–852.
[9] F. Wen, U. Simon, *Chem. Mater.* **2007**, *19*, 3370–3372.
[10] L. Zhang, B. Cheng, E. T. Samulski, *Chem. Phys. Lett.* **2004**, *398*, 505–510.
[11] J. C. Yu, X. L. Hu, Q. Li, Z. Zheng, Y. M. Xu, *Chem. Eur. J.* **2006**, *12*, 548–552.
[12] X.-W. Wei, G.-X. Zhu, C.-J. Xia, Y. Ye, *Nanotechnology* **2006**, *17*, 4307–4311.
[13] S. Shanmugam, A. Gedanken, *J. Phys. Chem. B* **2006**, *110*, 2037–2044.
[14] H. P. Klug, L. E. Alexander, *X-ray Diffraction Procedures*, Wiley, New York, **1959**.
[15] a) R. J. Nemanich, S. A. Solin, *Phys. Rev. B* **1979**, *20*, 392–401; b) R. P. Vidano, D. B. Fishbach, L. J. Willis, T. M. Loehr, *Solid State Commun.* **1981**, *39*, 341–344; c) S. M. Mominuzzaman, K. M. Krishna, T. Soga, T. Jimbo, M. Umeno, *Carbon* **2000**, *38*, 127–131.
[16] a) F. Zhang, J. Chen, X. Zhang, W. Gao, R. Gin, J. Gaun, Y. Li, *Langmuir* **2005**, *21*, 9329–9334; b) J. Prabhuram, X. Wang, C. L. Hui, I.-M. Hsing, *J. Phys. Chem. B* **2003**, *107*, 11057–11064.
[17] H. Ago, T. Kugler, F. Cacilli, W. R. Salanceck, M. S. P. Shaffer, A. H. Windle, R. H. Friend, *J. Phys. Chem. B* **1999**, *103*, 8116–8121.
[18] Y. Xie, P. M. A. Sherwood, *Appl. Spectrosc.* **1989**, *43*, 1153–1158.
[19] K. McCrea, J. Parker, G. Somorjai, *J. Phys. Chem. B* **2002**, *106*, 10854–10863.
[20] Z. Hu, F. M. Allen, C. Z. Wan, R. M. Heck, J. J. Steger, R. E. Lakis, C. E. Lyman, *J. Catal.* **1998**, *174*, 13–21.
[21] J. Gavillet, A. Loiseau, F. Ducastelle, S. Thair, P. Bernier, O. Stephan, *Carbon* **2002**, *40*, 1649–1663.

Received: June 25, 2008
Published online: August 19, 2008

